Structure−Function Analysis of a Series of Novel GIP Analogues Containing Different Helical Length Linkers†

Susanne Manhart,‡ Simon A. Hinke,§ Christopher H. S. McIntosh,§ Raymond A. Pederson,§ and Hans-Ulrich Demuth*,‡

Department of Peptide Chemistry, probiodrug AG, Weinbergweg 22, 06120 Halle/Saale, Germany, and Department of Physiology, Faculty of Medicine, University of British Columbia, 2146 Health Sciences Mall, Vancouver, BC, Canada V6T 1Z3

Received September 18, 2002; Revised Manuscript Received December 20, 2002

ABSTRACT: Glucose-dependent insulinotropic polypeptide (GIP_{1-42}) is a potent glucose-lowering intestinal peptide hormone. The equipotent $GIP_{1-30NH2}$ was structurally modified by linking N- and C-terminal fragments with several different linkers. Substitution of the middle region of GIP by a flexible aminohexanoic linker resulted in greatly reduced binding affinity and reduction or complete loss of bioactivity. Connection of the bioactive domains GIP_{1-14} and $GIP_{19-30NH2}$ by EKEK or AAAA linkers resulted in peptide agonists with approximately 3−4-fold increased bioactivity as compared to $GIP_{1-30NH2}$. Conformational analysis by CD spectroscopy of GIP fragments and analogues suggests a helical region in the C-terminal (19−30) portion of GIP. It was demonstrated that stabilization of this C-terminal helical region by the introduction of helical linkers favored binding and activation of the GIP receptor. Our results suggest an important contribution of a direct interaction of the first 14 amino acids with the GIP receptor, an appropriate relative orientation of N- and C-terminal parts of GIP, and the presence of helical linkers to be essential for bioactivity.

After oral glucose ingestion, the insulin response is much greater than after i.v.[1] glucose injection despite identical glycaemic conditions. This so-called incretin effect is mediated in a strictly glucose-dependent manner by two gastrointestinal hormones, GIP (glucose-dependent insulinotropic polypeptide) and GLP-1 (glucagon-like peptide 1), acting as signals from the gut to pancreatic β-cells (*1*, *2*) (Table 1). The 42 amino acid peptide hormone GIP is released from intestinal endocrine K cells after absorption of either glucose or fat (*3*). In addition to its glucose lowering action, GIP stimulates proinsulin gene expression, β-cell proliferation, and promotes β-cell survival (*4*, *5*). GIP also exerts metabolic actions on adipocytes (*6*, *7*). Recently, it was suggested from studies on GIP-receptor knockout (GIPR) mice that GIP may link overnutrition to obesity (*8*), opening a new therapeutic field for GIP antagonists as anti-obesity drugs.

Because of their insulinotropic actions, there is considerable interest in the therapeutic potential of both incretins in the treatment of diabetes mellitus, but the fast enzymatic degradation of GIP and GLP-1 by dipeptidyl peptidase (DP) IV is one shortcoming affecting their use as drug candidates (*9*−*11*). The use of cleavage resistant N-terminally modified peptides (*12*−*16*) and the application of DP IV inhibitors (*17*−*20*) are two approaches that have been utilized to prolong the biological half-life of these peptides. One potential drawback to the development of GIP analogues for the treatment of type 2 diabetes is an end organ resistance to GIP action that has been demonstrated in human infusion studies (*21*, *22*). However, studies in glucose intolerant rodents demonstrated that bolus injections of pharmacological amounts of GIP or DP IV-resistant analogues resulted in robust insulin responses and greatly improved glycaemic excursions (*16*, *23*). Despite this potential for GIP analogues in the treatment of both diabetes and obesity, the lack of orally administrable forms results in the challenging task of deriving small nonpeptide ligands from long-chain peptide hormones by rational drug design. A prerequisite for such design is a deeper understanding of the three-dimensional structure of GIP and structural parameters that contribute to its receptor interaction and bioactivity.

† This study was funded in part by the Department of Science and Technology of Saxony-Anhalt (Grant 9704/00116), the Federal Department of Science and Technology (Grant 0312302), and the Canadian Institutes of Health Research (Grant 590007).

* To whom correspondence should be addressed. Tel.: +49 345 5559900. Fax: +49 345 5559901. E-mail: Hans-Ulrich.Demuth@probiodrug.de.

‡ probiodrug AG.

§ University of British Columbia.

[1] Abbreviations: Symbols and abbreviations are in accordance with recommendations of the IUPAC−IUB commission on Biochemical nomenclature. All amino acids are of the L-configuration unless otherwise stated. Others: A, alanine; Ahx, amino hexanoic acid; BSA, bovine serum albumin; cAMP, 3′,5′-cyclic adenosine monophosphate; CD, circular dichroism; CHO-K1 cells, chinese hamster ovary-K1 cells; cpm, counts per minute; CRF, corticotropin releasing factor; DMEM, Dulbecco's modified Eagle's medium; DMF, dimethylformamide; DP IV, dipeptidyl peptidase IV; E, glutamic acid; EDTA, ethylenediamine tetraacetic acid; Fmoc, 9-fluorenylmethoxycarbonyl; GIP, glucose-dependent insulinotropic polypeptide; GIPR, GIP receptor; GLP-1, glucagon-like peptide 1; HEPES, 2-[4-(2-hydroxyethyl)-1-piperazinyl]-ethansulfonic acid; HPLC, high-performance liquid chromatography; IBMX, isobutylmethylxanthine; i.v., intravenous; K, lysine; KIU, kallikrein inhibitory units; MALDI, matrix-assisted laser desorption ionization time-of-flight mass spectrometry; Mol. $Ellip._{MRW}$, mean residue weight molar ellipticity; NMR, nuclear magnetic resonance spectroscopy; NPY, neuropeptide Y; wtGIPR cells, wild-type GIP receptor cells; TFA, trifluoroacetic acid; TFE, trifluoroethanol.

10.1021/bi026868e CCC: $25.00
Published on Web 02/20/2003

Table 1: Comparison of the Primary Amino Acid Sequences of GIP and GLP-1 from Humans

peptide	sequence
GIP	YAEGTFISDYSIAMDKIHQQDFVNWLLAQKGKKNDWKHNITQ
GLP-1[$_{7-36}$NH$_2$]	HAEGTFTSDVSSYLEGQAAKEFIAWLVKGR$_{NH2}$

The GIP receptor is a seven transmembrane G-protein coupled receptor belonging to the glucagon-secretin (B) family (*24*). GIP has been shown to increase adenylyl cyclase activity, elevate intracellular Ca^{2+} levels, and stimulate a mitogen-activated protein (MAP) kinase pathway in the pancreatic β-cell (*25*, *26*). In previous studies, it was shown that GIP$_{1-30NH2}$ has comparable insulinotropic activity to GIP$_{1-42}$ but reduced somatostatinotropic activity (*27*). With the cloned rat GIP receptor, GIP$_{1-42}$ and GIP$_{1-30NH2}$ were indistinguishable with respect to cAMP production and binding affinity (*28*). Recently, a series of truncated GIP analogues was synthesized for the purpose of elucidating the bioactive domain of GIP. In this study, it was shown that i.v. infusion of GIP$_{1-14}$ or GIP$_{19-30NH2}$ had similar glucose-lowering effects to GIP$_{1-42}$ in vivo, although at a 100-fold greater dosage (*28*). These results support the hypothesis of a one-receptor two-interaction-site mechanism, which was shown, for example, for peptides of the corticotropin releasing factor (CRF) family (*29*).

In the current study, N- and C-terminal binding domains of GIP$_{1-30NH2}$ were connected by linkers of variable length and structure based on those utilized by Beyermann et al. (*29*) in a study on CRF analogues. These new GIP analogues were tested on Chinese hamster ovary (CHO-K1) cells transfected with the wild-type rat pancreatic GIP receptor (wtGIPR cells). Biological activity of peptides was assessed by measurement of intracellular cAMP in transfected cells, while binding affinity was determined by competitive radioligand binding assays. The results from the functional studies of all analogues were correlated with the conformational properties arising from a secondary structure analysis by circular dichroism (CD) spectroscopy.

EXPERIMENTAL PROCEDURES

Preparation of Peptides. Peptides were produced with an automated synthesizer (Symphony; Rainin Instrument Co., USA) using a modified Fmoc protocol. Cycles were modified by using 5-fold excess of Fmoc amino acids (Novabiochem, Germany) and coupling reagent for 30 min in dimethylformamide (DMF; Roth, Germany). From the 10th amino acid, coupling times were extended up to 2 × 30 min, and depending on the peptide sequence, from the 25th amino acid up to 2 × 60 min. The peptide couplings were performed by 2-(1H-benzotriazole-1-yl)-1,1,3,3-tetramethyluronium tetrafluoroborate (TBTU; Novabiochem, Germany)/*N*-methylmorpholine (Merck, Germany) activation using a 0.23 mmol substituted NovaSyn TGR resin (Novabiochem, Germany) or, for synthesis of GIP$_{1-42}$ and the shorter N-terminal fragments, by using the preloaded Fmoc amino acid NovaSyn TGA resin (loading approximately 0.2 mmol/g; Novabiochem, Germany) at a 25 μmol scale. Fmoc deprotection was accomplished with 20% piperidine (Merck, Germany) in DMF (2 × 5 min and from the 25th coupling 2 × 10 min). Removal from the resin was carried out by a cleavage cocktail consisting of 94% trifluoroacetic acid (TFA; Merck, Germany), 2.5% water, 2.5% ethanedithiol (Merck, Germany), and 1% triisopropylsilane (Fluka, Switzerland).

Analytical and preparative HPLC was performed using different gradients on the LiChrograph HPLC system (Merck−Hitachi, Germany). The gradients were made from two solvents: (A) 0.1% TFA in H_2O and (B) 0.1% TFA in acetonitrile (Merck, Germany). Analytical HPLC was performed on a 125-4 LiChrospher RP18 column (Merck, Germany). Purification of the peptides was carried out by preparative HPLC on either a 250-20 Nucleosil 100 RP8 column (Macherey Nagel, Germany) or a 250-10 LiChrospher 300 RP18 column (flow rate 6 mL/min, detection at λ = 220 nm; Merck, Germany) under various conditions depending on peptide chain length.

Identity and purity were further assessed by matrix-assisted laser desorption ionization time-of-flight mass spectrometry (Hewlett-Packard G2025, Germany). Measured and expected masses are indicated in Table 2. This peptide synthesis protocol has been previously published (*15*, *28*).

CD Spectroscopy. The CD spectra were recorded on a JASCO J715 spectropolarimeter at 22 °C over a range of 185−250 nm in a nitrogen atmosphere. Weighed amounts of peptides were dissolved in phosphate buffer (20 mM, pH 7) to produce stock solutions of approximately 400 μM that were further diluted. The final concentrations (50−80 μM) were determined by UV using the absorbance at 280 nm. Samples were measured in a sample cell of 1 mm optical path length by accumulation of 15 scans. All spectra were corrected by subtraction of the buffer spectrum. Instrumental parameters were chosen as follows: response time, 2 s; sensitivity, standard; bandwidth, 2 nm; data pitch, 0.2 nm; and scanning speed, 20 nm/min. Calculation of the helical content was carried out according to Kallenbach et al. (*30*).

Cell Culture. The Chinese hamster ovary (CHO-K1) cells stably transfected with a eukaryotic expression plasmid (pcDNA3; Invitrogen, USA) containing the cDNA of the wild-type rat pancreatic islet GIP receptor (wtGIPR cells) have been previously described (*16*, *28*). Cells were grown in DMEM/F12 nutrient mixture supplemented with 10% newborn bovine serum, antibiotics, and 0.8 mg/mL G418 as the selection agent (all cell culture reagents were from Gibco Life Sciences, Canada). Cells were harvested by trypsin/EDTA treatment and dispensed at 50 000 cells per well in 24 well plates; after 2 days of culture, each well contained (2−4) × 10^5 cells to be used in cyclic AMP stimulation and binding competition experiments.

Cyclic AMP and Competitive Binding Studies. Experiments were carried out as previously described (*16*, *28*). For cAMP stimulation experiments, cells were washed twice in 37 °C assay buffer (15 mM HEPES-buffered DMEM/F12 with 0.1% BSA; HEPES and BSA from Sigma Chemical Co., USA) and allowed to preincubate for 1 h in this solution. Stimulation proceeded for 30 min in the same buffer additionally supplemented with 0.5 mM IBMX (Research Biochemicals Intl., USA), 100 KIU aprotinin (Trasylol; Bayer, Canada), and peptide at the concentrations indicated in the figures. Intracellular cAMP was extracted in ice cold 70% ethanol, and after removal of cell debris and drying,

Table 2: Summary Statistics for Cyclic AMP Production and Competitive Binding Displacement Studies on Synthetic GIP Fragments Using CHO-K1 Cells Transfected with the Rat GIP Receptor[a]

		Molecular Weight (Da)		cAMP production		Receptor Binding	
	synthetic peptide	expected	measured	max cAMP[b,c] (fold basal)	EC_{50}	% displacement at 20 μM	IC_{50}
0	$GIP_{1-30NH2}$	3552.0	3553.3	130 ± 11	271 ± 30 pM	100[d]	4.24 ± 0.39 nM
1	$GIP_{(1-6)(19-30)NH2}$	2157.6	2158.8	1.81 ± 0.42[e]		88.2 ± 0.7	2.74 ± 0.37 μM
2	$GIP_{(1-6)(AAAA)(19-30)NH2}$	2441.8	2440.5	7.21 ± 0.99[e]		88.7 ± 3.0	2.41 ± 0.46 μM
3	$GIP_{(1-6)(EKEK)(19-30)NH2}$	2672.1	2674.1	8.17 ± 0.87[e]		86.8 ± 1.6	2.09 ± 0.23 μM
4	$GIP_{(1-6)(EKEEKEKEEKE)(19-30)NH2}$	3574.0	3575.9	84.9 ± 8.1[e]	8.39 ± 0.18 μM[e,f]	75.1 ± 2.7	4.27 ± 0.14 μM
5	$GIP_{(1-6)(EKEEKEKEEKEK)(19-30)NH2}$	3702.3	3703.7	15.2 ± 3.1[e]		66.1 ± 1.2	3.32 ± 0.66 μM
6	$GIP_{(1-6)(Ahx)1(19-30)NH2}$	2270.7	2271.7	95.9 ± 8.6[e]	14.5 ± 4.7 μM[e,f]	62.0 ± 4.3	8.73 ± 2.24 μM
7	$GIP_{(1-6)(Ahx)2(19-30)NH2}$	2383.8	2386.0	2.55 ± 0.84[e]		75.3 ± 3.3	4.98 ± 0.40 μM
8	$GIP_{(1-6)(Ahx)3(19-30)NH2}$	2497.0	2498.8	13.5 ± 1.5[e]		67.1 ± 1.0	4.03 ± 0.64 μM
9	$GIP_{(1-14)(19-30)NH2}$	3038.6	3040.6	127 ± 22	78.7 ± 2.3 nM[e]	95.4 ± 0.7	1.37 ± 0.06 μM
10	$GIP_{(1-14)(AAAA)(19-30)NH2}$	3322.9	3322.7	82.1 ± 2.8[e]	58.7 ± 2.7 pM[e]	100.0 ± 0.9	66.3 ± 7.5 nM
11	$GIP_{(1-14)(EKEK)(19-30)NH2}$	3553.2	3551.6	80.6 ± 5.6[e]	77.0 ± 6.1 pM[e]	98.7 ± 1.1	26.0 ± 1.6 nM
12	$[D\text{-}Ala^2]GIP_{(1-14)(EKEK)(19-30)NH2}$	3553.2	3554.5	110 ± 15[e]	5.24 ± 0.61 nM[e]	99.0 ± 0.6	56.1 ± 2.5 nM
13	$GIP_{(1-14)(Ahx)1(19-30)NH2}$	3151.6	3155.6	102 ± 5	1.41 ± 0.32 μM[e,f]	86.1 ± 1.9	2.71 ± 0.23 μM
14	$GIP_{(1-14)(Ahx)2(19-30)NH2}$	3264.9	3264.8	95.9 ± 3.2[e]	2.51 ± 0.25 μM[e,f]	85.8 ± 1.6	2.77 ± 0.14 μM
15	$GIP_{(1-14)(Ahx)3(19-30)NH2}$	3378.0	3380.2	49.5 ± 1.6[e]	~20 μM[e,f]	82.7 ± 3.2	3.21 ± 0.44 μM

[a] Data represent mean ± SEM of three independent experiments. [b] Basal cyclic AMP = 2.680 ± 0.104 fmol/1000 cells. [c] Cyclic AMP stimulated by 20 μM peptide, if plateau levels were not achieved. [d] By definition, 1 μM $GIP_{1-30NH2}$ displaces all specific ^{125}I-GIP binding. [e] $p < 0.05$. [f] Estimated using maximal $GIP_{1-30NH2}$-stimulated cAMP.

cAMP was measured by radioimmunoassay (Biomedical Technologies Inc., USA).

Whole cell binding studies were initiated by washing cells twice with ice cold assay buffer, followed by addition of the same media with aprotinin, 50 000 cpm ^{125}I-GIP, and appropriate peptide concentrations. Equilibrium binding was achieved during overnight incubation (12−16 h, 4 °C), then cells were washed twice with cold assay buffer, solubilized in 0.2 N NaOH, and transferred to test tubes for counting cell associated radioactivity.

Data Analysis. Each experiment consisted of triplicate determinations, and a minimum of three independent experiments (cyclic AMP stimulation and binding study) were conducted for each peptide; data represent the mean ± SEM of three or more experiments. Cyclic AMP data were normalized to the maximal cAMP level obtained by stimulation with native hormone for each experiment, presented as a percent of this value. They are also provided as fold-basal values to clarify if any minor bioactivity was present in less potent analogues. Binding data are presented as a percentage of binding in the absence of competitor ($\%B/B_0$), and nonspecific binding was estimated as the binding in the presence of 1 μM GIP. Significance of differences was assessed by analysis of variance (ANOVA) and Dunett's *t* test, with a 5% significance level.

RESULTS

Two sets of $GIP_{1-30NH2}$ analogues were designed based on the previously characterized bioactive domains of GIP located in amino acid sequences 1−14 and 19−30 (*28*). In a first set of analogues, the bioactive N-terminal (1−14) domain was linked to the bioactive C-terminal (19−30) domain directly, either by deleting the intervening four amino acids or by introduction of different lengths of linkers (analogues 9−15, Table 2). In a second set of analogues, the N-terminal domain was reduced to the GIP (1−6) fragment, which alone shows no receptor binding or bioactivity, linked to the C-terminal (19−30) domain, in a manner similar to that described above and resulting in analogues 1−8 (Table 2). Similar to a strategy applied to CRF peptides (*29*), peptidic charged EK linkers (peptides 3−5, 11, and 12), a peptidic uncharged poly-Ala linker (peptides 2 and 10), both of which should favor a helical conformation, and a flexible uncharged aminohexanoic linker (Ahx) were introduced into GIP analogues (peptides 6−8 and 13−15). For analogues 10, 11, and 12 (Table 2), the four amino acids of the natural sequence were replaced by an EKEK or an AAAA linker. In the second set of analogues, the same EKEK/AAAA linker was tested as well as a longer EK linker to obtain the original length of the $GIP_{1-30NH2}$ peptide. In both sets of analogues, different lengths of the $(Ahx)_n$ linker ($n = 1-3$) were tested.

All analogues were tested for their receptor binding affinity and ability to stimulate adenylyl cyclase in CHO-K1 cells transfected with the wtGIP receptor (Table 2). Concerning the dependence of their secondary structure on the deletion of amino acids or the introduction of several linker structures, aqueous solutions of the analogues were investigated by CD spectroscopy. The spectra were analyzed according to their $-[\Theta]_{222}$ values (mean residue weight molar ellipticity at 222 nm) (*30*) and presented as % α-helix (*f*) in Tables 3 and 4.

In the binding experiments, native $GIP_{1-30NH2}$ was able to displace 50% of ^{125}I-GIP_{1-42} binding in the nanomolar range (IC_{50} = 4.24 ± 0.39 nM), whereas all of the tested peptide analogues showed IC_{50} values in the low micromolar range (2−9 μM) except analogues 10−12 exhibiting IC_{50} values of 66.3 ± 7.5, 26 ± 1.6, and 56.1 ± 2.5 nM, respectively. This corresponds to a 6−15-fold reduction in affinity of the analogues as compared to $GIP_{1-30NH2}$. In general, all peptides based on N-terminal GIP_{1-6} sequences, deletion analogues, and peptides with flexible Ahx linkers displayed 500−2000-fold reduced binding affinity (Table 2, Figure 1).

All analogues were tested for agonist properties on wtGIPR cells. The resulting maximal cAMP and EC_{50} values are compiled in Table 2. Full concentration−response curves of all tested analogues are presented in Figure 2. None of

Table 3: Helix Content of GIP and GIP Analogues in 20 mM Phosphate Buffer at pH 7

number	peptide	$-[\Theta]_{222}$[a]	f (%)[b]
	GIP_{1-42}	4550	11
	$GIP_{1-30NH2}$	3360	8.5
	$GIP_{19-30NH2}$	5043	17
1	$GIP_{(1-6)(19-30)NH2}$	4620	13.5
2	$GIP_{(1-6)(AAAA)(19-30)NH2}$	4455	12
3	$GIP_{(1-6)(EKEK)(19-30)NH2}$	4098	11
4	$GIP_{(1-6)(EKEEKEKEEKE)(19-30)NH2}$	6573	18
5	$GIP_{(1-6)(EKEEKEKEEKEK)(19-30)NH2}$	8313	23
6	$GIP_{(1-6)(Ahx)1(19-30)NH2}$	3474	9.5
7	$GIP_{(1-6)(Ahx)2(19-30)NH2}$	4859	14
8	$GIP_{(1-6)(Ahx)3(19-30)NH2}$	3218	8.5
9	$GIP_{(1-14)(19-30)NH2}$	7229	20
10	$GIP_{(1-14)(AAAA)(19-30)NH2}$	4512	12
11	$GIP_{(1-14)(EKEK)(19-30)NH2}$	5473	14.5
12	$[D\text{-}Ala^2]GIP_{(1-14)(EKEK)(19-30)NH2}$	5850	16
13	$GIP_{(1-14)(Ahx)1(19-30)NH2}$	4211	11
14	$GIP_{(1-14)(Ahx)2(19-30)NH2}$	2421	6
15	$GIP_{(1-14)(Ahx)3(19-30)NH2}$	3042	8

[a] $-[\Theta]_{222}$, mean residue ellipticity (deg cm^2/dmol) of peptides at 222 nm. [b] f = fraction of helix, was calculated according to $f = [\Theta]_{obs} - [\Theta]_0/[\Theta]_{max} - [\Theta]_0$. $[\Theta]_{obs}$ measured $[\Theta]_{222}$ value. $[\Theta]_0 = -500$ deg cm^2/dmol. $[\Theta]_{max} = (1 - 4/n)[\Theta]_H$ = the maximal mean residue ellipticity value for chain length, where n = the number of residues and $[\Theta]_H = -40\,000$ deg cm^2/dmol.

Table 4: Helix Content of GIP and GIP Analogues in 20 mM Phosphate Buffer at pH 7 Containing 40% Trifluoroethanol

number	peptide	$-[\Theta]_{222}$[a]	f (%)[b]
	GIP_{1-42}	28 716	79
	$GIP_{1-30NH2}$	15 738	45
10	$GIP_{(1-14)(AAAA)(19-30)NH2}$	27 887	80
11	$GIP_{(1-14)(EKEK)(19-30)NH2}$	16 369	47
13	$GIP_{(1-14)(Ahx)1(19-30)NH2}$	9746	28

[a] $-[\Theta]_{222}$, mean residue ellipticity (deg cm^2/dmol) of peptides at 222 nm. [b] f = fraction of helix, was calculated according to $f = [\Theta]_{obs} - [\Theta]_0/[\Theta]_{max} - [\Theta]_0$. $[\Theta]_{obs}$ measured $[\Theta]_{222}$ value. $[\Theta]_0 = 0 \pm 500$ deg cm^2/dmol. $[\Theta]_{max} = (1 - 4/n)[\Theta]_H$ = the maximal mean residue ellipticity value for chain length, where n = the number of residues and $[\Theta]_H = -40\,000$ deg cm^2/dmol.

the analogues 1−3, 5, 7, and 8, in which the N-terminal GIP_{1-6} fragment was connected to $GIP_{19-30NH2}$ directly or via the EKEK/AAAA or Ahx_n linker (n = 2, 3), were able to stimulate maximal cAMP production (Figure 2B). Only analogue 4 with the longer 11-membered EK linker and analogue 6, with the (1−6) fragment connected by one Ahx residue, showed potent increases in cAMP from basal levels indicating that a minimum length of the peptide is necessary for bioactivity. The EC_{50} values of analogues 4 and 6 were in the micromolar range; however, both analogues appear to be full agonists (Table 2). Analogue 5, differing from analogue 4 only by the introduction of an additional lysine to achieve a length of 30 amino acids, demonstrated a complete loss of bioactivity (Table 2, Figure 2B).

Analogues resulting from the connection of (1−14) and (19−30) domains by one or two Ahx residues (analogues 13 and 14, respectively) showed noticeable increases in cAMP production with EC_{50} values in the low micromolar range, similar to analogues 4 and 6 (Table 2, Figure 2A). The introduction of an extra Ahx residue (analogue 15) resulted in nearly complete loss of ability to stimulate cAMP production, perhaps because of excessive conformational freedom induced by three successive aminohexanoic acids

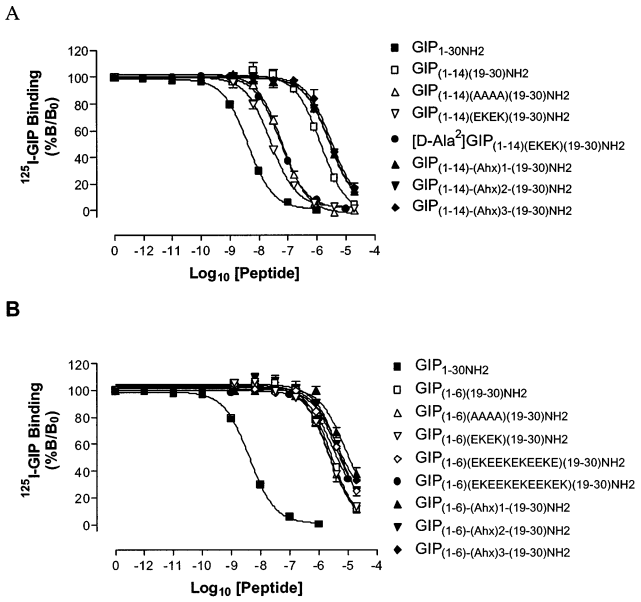

FIGURE 1: Competition-binding displacement curves of synthetic $GIP_{1-30NH2}$ analogues and ^{125}I-GIP on CHO-K1 cells transfected with the wild-type rat GIP receptor (wtGIPR). (A) GIP_{1-14}-connecting analogues. (B) GIP_{1-6}-connecting analogues. Data represent the mean ± SEM of three or more independent experiments. Refer to Table 2 for binding statistics.

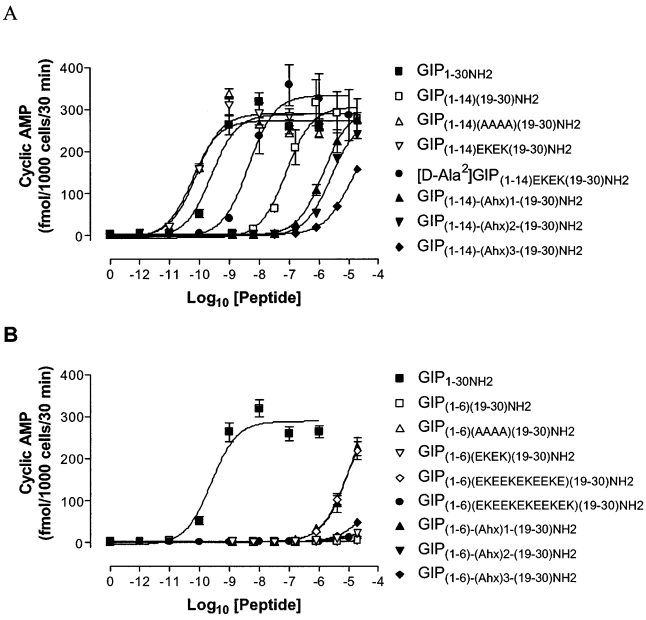

FIGURE 2: Concentration−response curve of intracellular cAMP production in wtGIPR cells by synthetic $GIP_{1-30NH2}$ analogues. (A) GIP_{1-14}-connecting analogues. (B) GIP_{1-6}-connecting analogues. Data represent the mean ± SEM of three or more independent experiments. Refer to Table 2 for cAMP stimulation statistics.

(Figure 2A). The direct connection of GIP_{1-14} to $GIP_{19-30NH2}$ (analogue 9) resulted in an analogue producing a large cAMP response with an EC_{50} of 78.7 ± 2.3 nM. The efficacy of analogues 10 and 11 (EC_{50} = 58.7 ± 2.7 and 77.0 ± 6.1 pM, respectively) was increased about 3−4-fold as compared to $GIP_{1-30NH2}$ (EC_{50} = 271 ± 30 pM; Table 2, Figure 2A). Thus, the AAAA and EKEK linkers seem to favor a conformation with enhanced bioactivity as compared to the native peptide. The DP IV-resistant analogue 12 was synthesized by introduction of D-alanine in position 2 in accordance with earlier work on DP IV-resistant GIP

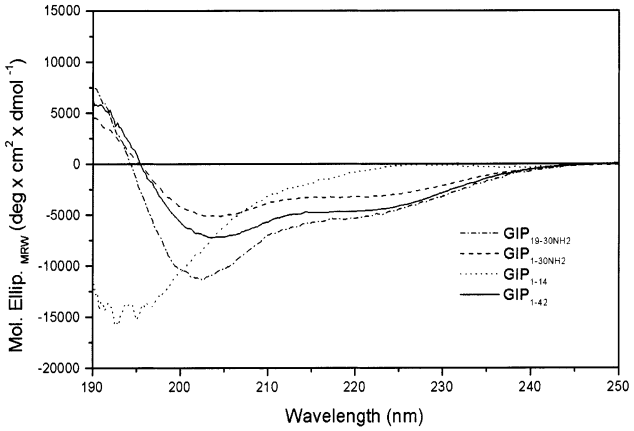

FIGURE 3: Representative CD spectra of selected synthetic GIP fragments. Each peptide was prepared and recorded at concentrations in the range of 60−80 μM in 20 mM phosphate buffer (pH 7) at 22 °C. For calculation of the helical content, refer to Table 3 and the text for more details.

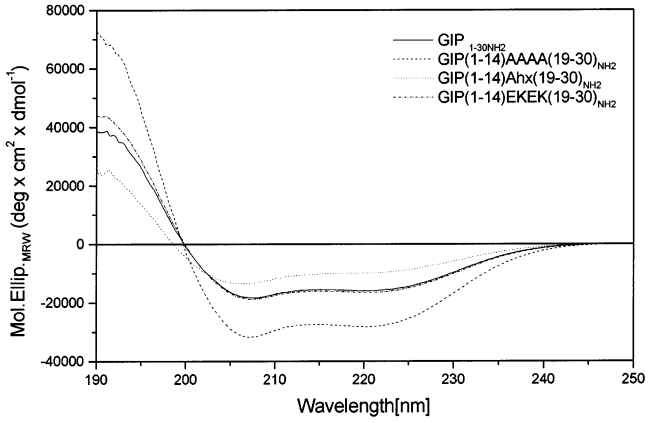

FIGURE 4: Representative CD spectra of selected synthetic $GIP_{1-30NH2}$ analogues. Each analogue was prepared and recorded at concentrations in the range of 60−80 μM in 20 mM phosphate buffer (pH 7) containing 40% TFE at 22 °C. For calculation of the helical content, refer to Table 4.

analogues (*15*, *16*). Despite the 68-fold reduction in in vitro bioactivity of analogue 12, when compared to analogue 11 (Table 2), it exhibits nearly the same binding affinity, and given the increased in vivo bioactivity observed for other DP IV-resistant analogues, it promises to be a very effective analogue for in vivo experiments (*14*, *16*).

Conformational analysis revealed only 8−11% helicity for $GIP_{1-30NH2}$ and GIP_{1-42} in aqueous buffer at pH 7 (Table 3, Figure 3). As expected, the shorter fragments GIP_{1-13} and GIP_{1-15} revealed a very similar set of CD spectra without a defined secondary structure (presented for GIP_{1-14} in Figure 3). Remarkably, for the short C-terminal fragment $GIP_{19-30NH2}$, the calculation of the helical content from the $-[\Theta]_{222}$ value resulted in 17% helix (Table 3, Figure 3). For the linker analogues, the helicity varied between 6 and 23% (Table 3). For most of the analogues with aminohexanoic residues as linkers, a helicity was calculated lower than 11% (Table 3). Substitution by linkers with a high helical propensity (the AAAA and EK linker) resulted effectively in an increase of helical content up to 23% (Table 3), but generally the differences between the $-[\Theta]_{222}$ values are relatively low in aqueous buffer. By addition of 40% trifluoroethanol, the helix−coil equilibrium of the peptides in aqueous solution was influenced in favor of the helical structure for a structural evaluation of the biological active GIP_{1-14} connected analogues 10 and 11 in comparison to $GIP_{1-30NH2}$ and the inactive analogue 13 (Figure 4). The helicity corresponding to the $-[\Theta]_{222}$ value of analogues 10 and 11 is significantly higher in contrast to the Ahx-connected analogue 13, indicating that the binding sites might be advantageously linked by a helical linker (Table 4, Figure 4).

DISCUSSION

GIP structure−activity studies have focused on identification of bioactive binding domains (*28*) and introduction of enzyme resistance by synthetic modifications on the N-terminus of GIP to prolong biological half-life while maintaining bioactivity (*14*−*16*, *31*, *32*). From these studies, it was demonstrated that the integrity of the N-terminus is important for receptor activation. Substitutions in positions 1−4 of $GIP_{1-30NH2}$ resulted in relatively minor changes in binding affinity but in dramatic effects on the ability to stimulate cAMP production. Nevertheless, very effective DP IV-resistant analogues exhibiting enhanced antihyperglycaemic activity, and insulin-releasing action in vivo could be identified (*14*, *16*). Additionally, GIP has been shown to be dissociable into two insulinotropic domains, GIP_{1-14} and $GIP_{19-30NH2}$, which appear to be full agonists with low binding affinities for the GIP receptor (*28*). It is thought that conformational changes within the peptide influence biological activity. Beyermann et al. (*29*) showed the role of different structured connectors and the preference for a helical structure for CRF analogues. In the current study, a similar approach was used to investigate the effect of changes in conformational freedom by introduction of flexible or helical linkers or amino acid deletion.

Reduction of the GIP N-terminal fragment to the first six amino acids and connection of this fragment directly to the (19−30) fragment (analogue 1) resulted in the complete loss of bioactivity and low binding affinity (Table 2, Figures 1B and 2B). Comparing analogue 1 with analogue 9 indicates that the amino acids 7−14 (-Ile-Ser-Asp-Tyr-Ser-Ile-Ala-Met-) are required for potent receptor activation. This is also supported by an alanine scanning study in vitro with GIP_{1-14}, where only the substitution of amino acid 4 is well-tolerated (S. Hinke and S. Manhart, unpublished data). Most of the (1−6)-connected analogues show little biological activity and binding affinities similar to that previously reported for the isolated C-terminal fragment $GIP_{19-30NH2}$ (Table 2, Figures 1B and 2B) (*28*). Only analogues with the 11-membered helical linker (analogue 4) and with one aminohexanoic residue (analogue 6) showed bioactivity with EC_{50} values in the micromolar range (Figure 2B). Assuming that 30 amino acids is the preferred size of the peptide, it was surprising that the 30 amino acid analogue 5, differing from analogue 4 by one extra lysine, is a relatively inactive analogue (Figure 2B). A combination of changed net charge of the linker with an unfavorable relative orientation of both binding sites could be an explanation. In analogue 6, the aminohexanoic residue seems to favor the conformational freedom of the peptide for the correct relative orientation of both binding sites. It can be concluded that an optimal distance and spatial orientation between N- and C-terminal parts of the peptide play major roles in receptor activation independently of the structural nature (helical or flexible)

of the linker. This is confirmed by secondary structure analysis of these low binding (1−6)-fragment analogues (Table 3). Similar to a study with neuropeptide Y (NPY) analogues (*33*), CD spectra of GIP analogues revealed no simple functional correlation between helical content (analogue 4: 18% helix and analogue 6: 9.5% helix) and bioactivity (Tables 2 and 3).

When GIP's N-terminal (1−14) and C-terminal (19−30) fragments were linked by the small intervening sequences EKEK and AAAA (analogues 10−12), the IC_{50} values shifted only approximately 10-fold as compared to the binding of native GIP to the receptor (Figure 1A). A similar binding behavior was observed if intervening GLP-1 sequences ($GLP\text{-}1_{12-18}$ and $GLP\text{-}1_{15-18}$) were introduced to GIP (S. Hinke and S. Manhart, manuscript in preparation). The cAMP data for these chimeric peptides showed the bioactivity of the two bioactive GIP domains to be additive. With analogues 10 and 11, bioactivity was increased as compared to $GIP_{1-30NH2}$ (Figure 2A), indicating that the EKEK and AAAA linker induce a particularly favored conformation. Thus, an optimal relative orientation between the two binding sites appears to have been achieved, and the nature of the amino acid side chains of the linker is not important for receptor interaction. Whether this effect is caused by induction of a more helical structure is questionable. In fact, secondary structure analysis under physiological conditions resulted in a slightly elevated helical content for analogues 10 and 11 (Table 3), but in the presence of 40% TFE the helix stabilizing effect of these linkers becomes evident (Table 4, Figure 4).

The deletion of the middle amino acids (analogue 9) and the introduction of aminohexanoic residues (analogues 13−15) resulted in binding affinities in the low micromolar range (Table 2, Figure 1A). But despite having low binding affinity, the deletion analogue 9 and analogues 13 and 14, with one and two Ahx residues, are full agonists comparable to analogues 4 and 6 (Figure 2A). This also indicates that for the (1−14)-connected analogues it is necessary to have a spacer between the two binding sites that provides both the correct distance and the correct relative orientation. It is likely that the aminohexanoic residues do not provide the appropriate distance and/or give too much conformational freedom to the analogues to obtain high affinity binding. Furthermore, the Ahx linker moieties do not mimic a peptide backbone. They create an achiral, more or less hydrophobic and highly versatile surface that may not be recognized by the receptor. Interestingly, even analogues (4, 6, 13, and 14) with greatly simplified peptide structures resulting in low binding affinities retain their intrinsic ability to activate the receptor.

The literature contains some structural studies for GIP-related peptide hormones such as glucagon, GLP-1, or exendin-4, a potent GLP-1-agonist, but not for GIP itself. For glucagon, the helical state has been established by X-ray crystallography (*34*). For GLP-1 and exendin-4, CD and NMR studies suggested a helical structure as the preferred conformational state for receptor interaction (*35*−*37*). For some peptide hormones that interact with the B-family of G-protein coupled receptors, a more flexible region between N- and C-terminal helical regions has been proposed as a structural prerequisite for receptor interaction (*38*, *39*). Therefore, the question arose as to whether the preferred conformational state for GIP/GIP receptor interaction is also a helical one. Our CD studies revealed that GIP_{1-42} and $GIP_{1-30NH2}$ are only about 10% helical in aqueous solution (pH 7, Table 3). Similarly, in the case of glucagon, only 15% helical structure and an unexpected high proportion of β-sheet was observed by CD in aqueous solution (*36*, *40*). Andersen et al. (*36*) observed a concentration and pH dependence of the helical content for GLP-1. At a pH of 3.5 in aqueous buffer the helical content of GLP-1 was relatively high, with 23% helix at 3.5 μM and 34% helix at 315 μM, when compared to pH 5.9, with 15% helix at 3.15 μM and 38% helix at 50 μM (*36*). We also observed a weak concentration dependence of the helical content for GIP_{1-42} at pH 7 in 20 mM phosphate buffer. In the concentration range between 10 and 60 μM, the helical content was calculated to be 6 and 11%, respectively.

It was demonstrated from studies on GLP-1 analogues that the ionic strength can also strongly influence the secondary structure content and self-aggregation tendency (*41*). It has also been shown that the bioavailability of peptide analogues, designed for therapeutic applications, depends strongly on their bioactive conformation, which is influenced by the formulation used (*41*). Generally, it can be assumed from CD and NMR studies for glucagon, GLP-1, and for GIP that these peptides are bioactive under physiological conditions as monomers existing in a preferred random coil state with a minor helical content. Under the more hydrophobic environment of their membrane bound receptors, these peptide hormones adopt their conformation to the biologically relevant and stable helical conformation (*42*). This is confirmed by several CD and NMR studies, showing that these peptides become more helical in media containing lipid micelles or other organic additives such as fluoro alcohols (*35*, *43*, *44*). The results of our own studies are in agreement with this hypothesis (Table 4, Figure 4).

We have compared the structural preferences of the linker analogues with native GIP. Deletion of the middle part of GIP (analogues 1 and 9) and the introduction of the AAAA and EK linker (analogues 2−5, 10, and 11) resulted in a noticeable increase in the helical content (Tables 3 and 4). Thus, it can be concluded that this type of linker supports the formation of a helical state in contrast to the Ahx linker analogues. Apart from these residues, it was clear from the deletion analogues 1 and 9 that the amino acids of the middle part of native GIP (residues 15−18 and 7−18) do not contribute to a helical structure. Therefore, the native linking sequence between the bioactive domain provides no additional contribution to helicity. As expected, the high affinity binding analogues 10 and 11, with increased bioactivity, are analogues that show a higher propensity for a helical structure (Table 2, Figure 4).

Conclusions from the CD spectra in aqueous solution have to be considered with care since it may not truly reflect the conformational state required for receptor interaction. A simple correlation between a distinct secondary structure and receptor interaction is not presently clear. NMR studies for both glucagon and GLP-1 in the micelle bound state (*43*, *44*) show a helical segment in the C-terminal part (residues 17/18−29) and a second helical segment for residues 10−14 in glucagon and residues 7−14 in GLP-1. On the basis of the observation that the C-terminal fragment $GIP_{19-30NH2}$ revealed a relatively high helical content in contrast to the N-terminal fragments (Table 3, Figure 3), we propose a

similar secondary structure for the C-terminal domain of $GIP_{1-30NH2}$, with a helical region similar to that found in glucagon and GLP-1. The short linker structures EKEK and AAAA possibly stabilize the helical C-terminal part of $GIP_{1-30NH2}$ and provide the optimal distance and orientation of the more flexible N-terminal part for receptor activation.

The current study has partially addressed hypotheses generated from prior structure−function relationships of GIP. Previously, use of computer algorithms to predict the helical nature of globular proteins was applied to GIP (*28*, *45*), predicting 52% helicity for GIP_{1-42} and 67% helicity for $GIP_{1-30NH2}$. This study is the first to report experimentally determined values, which calculated helical content for both peptides to be approximately 10% (Table 3) in aqueous solutions. In the presence of TFE, the helical content of $GIP_{1-30NH2}$ and GIP_{1-42} was calculated by CD spectroscopy to be 45 and 79%, respectively (Table 4). The discrepancy between the predicted and the measured values justifies further investigation of the structure of GIP by other methods. We previously presented data indicating two independent bioactive binding domains of GIP; cAMP production by GIP_{1-14} could not be antagonized by $GIP_{17-30NH2}$, whereas cAMP production by $GIP_{19-30NH2}$ could be antagonized by $GIP_{17-30NH2}$; thus, two separate binding sites were implicated. Additive effects of GIP_{1-14} and $GIP_{19-30NH2}$ were not demonstrated, as neither peptide was able to stimulate maximal cAMP production in wtGIPR cells, although EC_{50} values were estimated to be in the micromolar range (*28*). Here, it is shown that tethering the two bioactive domains together with no intervening sequence enhances potency, likely by overcoming entropy. Even greater potency is achieved by inserting nonspecific AAAA or EKEK linkers, likely by overcoming entropic effects and spatial requirements (Table 2).

In summary, in the current study we investigated the characteristics of novel $GIP_{1-30NH2}$ analogues consisting of N- and C-terminal fragments joined directly or with several different linkers. It is evident that modifications in the middle part of GIP affect bioactivity and conformation. For the (1−6)-connected analogues, receptor activation appears to be controlled by the nature of the side chains of the first 14 amino acids rather than by backbone conformation. It was demonstrated that an appropriate distance and relative orientation of the binding sites seem to be decisive factors for receptor activation. The introduction of amino acids with high helical propensity between the two binding sites GIP_{1-14} and $GIP_{19-30NH2}$ resulted in very potent GIP agonists. Finally, the introduction of DP IV resistance by modifications at the N-terminus of GIP in combination with the described conformational changes in the middle part of the peptide is suggested to result in promising candidates for further in vivo studies. This work provides information for a better understanding of GIP/GIP receptor interaction, may contribute to the development of highly selective receptor ligands, and further justifies the need to study the structure of GIP by NMR or crystallography.

ACKNOWLEDGMENT

We gratefully acknowledge the technical assistance of C. Schnittka and M. Speck. We thank Dr. A. Porzel and M. Süsse for providing the CD spectrometer and for the assistance in recording the CD spectra. We thank Drs. Ralph Golbik and Jens-Ulrich Rahfeld for critical reading of the manuscript and helpful discussions.

REFERENCES

1. Fehmann, H.-C., Göke, R., and Göke, B. (1995) *Endocr. Rev. 16*, 390−410.
2. Creutzfeldt, W. (2001) *Exp. Clin. Endocrinol. Diabetes 109*, S288−S303.
3. Pederson, R. A. (1994) in *Gut peptides*: *Biochemistry and Physiology* (Walsh, J. H., and Dockray, G. J., Eds.), pp 217−259, Raven Press, New York.
4. Ehses, J. A., Casilla, V., Pospisilik, J. A., Doty, T., Demuth, H.-U., Pederson, R. A., and McIntosh, C. H. S. (2002) *Diabetes 51 (Supplement 2)*, A339.
5. Trümper, A., Trümper, K., Trusheim, H., Arnold, R., Göke, B., and Hörsch, D. (2001) *Mol. Endocrinol. 15*, 1559−1570.
6. McIntosh, C. H. S., Bremsak, I., Lynn, F. C., Gill, R., Hinke, S. A., Gelling, R., Nian, C., McKnight, G., Jaspers, S., and Pederson, R. A. (1999) *Endocrinology, 140*, 398−404.
7. Yip, R. G., and Wolfe, M. M. (2000) *Life Sci. 66*, 91−103.
8. Miyawaki, K., Yamada, Y., Ban, N., Ihara, Y., Tsukiyama, K., Zhou, H., Fujimoto, S., Oku, A., Tsuda, K., Toyokuni, S., Hiai, H., Mizunoya, W., Fushiki, T., Holst, J. J., Makino, M., Tashita, A., Kobara, Y., Tsubamoto, Y., Jinnouchi, T., Jomori, T., and Seino, Y. (2002) *Nat. Med. 8*, 738−742.
9. Mentlein, R., Gallwitz, B., and Schmidt, W. E. (1993) *Eur. J. Biochem. 214*, 829−835.
10. Kieffer, T. J., McIntosh, C. H. S., and Pederson, R. A. (1995) *Endocrinology 136*, 3585−3596.
11. Pauly, R. P., Rosche, F., Wermann, M., McIntosh, C. H. S., Pederson, R. A., and Demuth, H.-U. (1996) *J. Biol. Chem. 271*, 23222−23229.
12. Deacon, C. F., Knudsen, L. B., Madsen, K., Wiberg, F. C., Jacobsen, O., and Holst, J. J. (1998) *Diabetologia 41*, 271−278.
13. Siegel, E. G., Gallwitz, B., Scharf, G., Mentlein, R., Morys-Wortmann, C., Fölsch, U. R., Schrezenmeir, J., Drescher, K., and Schmidt, W. E. (1999) *Regul. Pept. 79*, 93−102.
14. O'Harte, F. P. M., Mooney, M. H., and Flatt, P. R. (1999) *Diabetes, 48*, 758−765.
15. Kühn-Wache, K., Manhart, S., Hoffmann, T., Hinke, S. A., Gelling, R., Pederson, R. A., McIntosh, C. H. S., and Demuth, H.-U. (2000) *Adv. Exp. Med. Biol. 477*, 187−195.
16. Hinke, S. A., Gelling, R. W., Pederson, R. A., Manhart, S., Nian, C., Demuth, H.-U., and McIntosh, C. H. S. (2002) *Diabetes, 51*, 652−661.
17. Pauly, R. P., Demuth, H.-U., Rosche, F., Schmidt, J., White, H. A., Lynn, F., McIntosh, C. H. S., and Pederson, R. A. (1999) *Metabolism 48*, 385−389.
18. Deacon, C. F., Danielsen, P., Klarskov, L., Olesen, M., and Holst, J. J. (2001) *Diabetes 50*, 1588−1597.
19. Pederson, R. A., White, H. A., Schlenzig, D., Pauly, R. P., McIntosh, C. H. S., and Demuth, H.-U. (1998) *Diabetes 47*, 1253−1258.
20. Balkan, B., Kwasnik, L., Miserendino, R., Holst, J. J., and Li, X. (1999) *Diabetologia 42*, 1324−1331.
21. Elahi, D., McAloon-Dyke, M., Fukagawa, N. K., Meneilly, G. S., Sclater, A. L., Minaker, K. L., Habener, J. F., and Andersen, D. K. (1994) *Regul. Pept. 51*, 63−74.
22. Nauck, M. A., Heimesaat, M. M., Ørskov, C., Holst, J. J., Ebert, R., and Creutzfeldt, W. (1993) *J. Clin. Invest. 91*, 301−307.
23. O'Harte, F. P. M., Mooney, M. H., Kelly, C. M., and Flatt, P. R. (2000) *J. Endocrinol. 165*, 639−648.
24. Usdin, T. B., Mezey, É., Button, D. C., Brownstein, M. J., and Bonner, T. I. (1993) *Endocrinology 133*, 2861−2870.
25. McIntosh, C. H. S., Wheeler, M. B., Gelling, R. W., Brown, J. C., and Pederson, R. A. (1996) *Acta Physiol. Scand. 157*, 361−365.
26. Ehses, J. A., Lee, S. S., Pederson, R. A., and McIntosh, C. H. S. (2001) *J. Biol. Chem. 276*, 23667−23673.
27. Morrow, G. W., Kieffer, T. J., McIntosh, C. H. S., MacGillivray, R. T. A., Brown, J. C., St. Pierre, S., and Pederson, R. A. (1996) *Can. J. Physiol. Pharmacol. 74*, 65−72.
28. Hinke, S. A., Manhart, S., Pamir, N., Demuth, H.-U., Gelling, W., Pederson, R. A., and McIntosh, C. H. S. (2001) *Biochim. Biophys. Acta 1547*, 143−155.

29. Beyermann, M., Rothemund, S., Heinrich, N., Fechner, K., Furkert, J., Dathe, M., Winter, R., Krause, E., and Bienert, M. (2000) *J. Biol. Chem. 275*, 5702−5709.
30. Kallenbach, N. R., Lyu, P., Hougxing, Z. (1996) in *Circular dichroism and the conformational analysis of biomolecules* (Fasman, G. D., Ed.) pp 201−259, Plenum Press, New York.
31. Gault, V. A., O'Harte, F. P. M., Harriott, P., and Flatt, P. R. (2002) *Biochem. Biophys. Res. Commun. 290*, 1420−1426.
32. Hinke, S. A., Gelling, R., Manhart, S., Lynn, F., Pederson, R. A., Kühn-Wache, K., Rosche, F., Demuth, H.-U., and McIntosh, C. H. S. (2003) *Biol. Chem. 384*(3), in press.
33. Soll, R. M., Dinger, M. C., Lundell, I., Larhammer, D., and Beck-Sickinger, A. G. (2001) *Eur. J. Biochem. 268*, 2828−2837.
34. Sasaki, K., Dockerill, S., Adamiak, D. A., Tickle, I. J., and Blundell, T. (1975) *Nature 257*, 751−757.
35. Parker, J. C., Andrews, K. M., Rescek, D. M., Massefski, W. J., Andrews, G. C., Contillo, L. G., Stevenson, R. W., Singleton, D. H., and Suleske, R. T. (1998) *J. Pept. Res. 52*, 398−409.
36. Andersen, N. H., Brodsky, Y., Neidigh, J. W., and Prickett, K. S. (2002) *Bioorg. Med. Chem. 10*, 79−85.
37. Neidigh, J. W., Fesinmeyer, R. M., Prickett, K. S., and Andersen, N. H. (2001) *Biochemistry 40*, 13188−13200.
38. Pellegrini, M., Royo, M., Rosenblatt, M., Chorev, M., and Mierke, D. F. (1998) *J. Biol. Chem. 273*, 10420−10427.
39. Barden, J. A., and Kemp, B. E. (1993) *Biochemistry 32*, 7126−7132.
40. Trivedi, D., Lin, Y., Ahn, J. M., Siegel, M., Mollova, N. N., Schram, K. H., and Hruby, V. J. (2000) *J. Med. Chem. 43*, 1714−1722.
41. Clodfelter, D. K., Pekar, A. H., Rebhun, D. M., Destrampe, K. A., Havel, H. A., Myers, S. R., and Brader, M. L. (1998) *Pharm. Res. 15*, 254−262.
42. Inooka, H., Ohtaki, T., Kitahara, O., Ikegami, T., Endo, S., Kitada, C., Ogi, K., Onda, H., Fujino, M., Shirakawa, M. (2001) *Nat. Struct. Biol. 8*, 161−165.
43. Thornton, K., and Gorenstein, D. G. (1994) *Biochemistry 33*, 3532−3539.
44. Braun, W., Wider, G., Lee, K. H., and Wüthrich, K. (1983) *J. Mol. Biol. 169*, 921−948.
45. Gelling, R. W., Coy, D. H., Pederson, R. A., Wheeler, M. B., Hinke, S., Kwan, T., McIntosh, C. H. S. (1997) *Regul. Pept. 69* (3), 151−154.

BI026868E